

Desorption kinetics of alkali atoms from transition metals

This article has been downloaded from IOPscience. Please scroll down to see the full text article.

1997 J. Phys.: Condens. Matter 9 9469

(<http://iopscience.iop.org/0953-8984/9/44/004>)

View [the table of contents for this issue](#), or go to the [journal homepage](#) for more

Download details:

IP Address: 171.66.16.209

The article was downloaded on 14/05/2010 at 10:55

Please note that [terms and conditions apply](#).

Desorption kinetics of alkali atoms from transition metals

R O Unãc†, J L Sales†, M V Gargiulo† and G Zgrablich‡

† Instituto de Energía Eléctrica y Departamento de Geofísica y Astronomía, Universidad Nacional de San Juan, Argentina

‡ Departamento de Física, Centro Latinoamericano de Estudios Ilya Prigogine, Universidad Nacional de San Luis, Chacabuco 917, 5700 San Luis, Argentina

Received 21 March 1997, in final form 4 August 1997

Abstract. A model for the adsorption of alkali atoms on transition metals is proposed and thermal desorption spectra are analysed for the systems K/Ni(111), K/Pt(111) and K/Fe(111). The basic assumption is that the interaction energy between alkali atoms, being of dipole–dipole type, attenuates as coverage increases. The attenuation function, obtained by fitting experimental thermal desorption spectra, is used to calculate the variation with coverage of the dipole moment and the work function through the Topping model. These calculations show an excellent agreement with independent experimental measurements of the dipole moment and work function over the whole coverage range.

1. Introduction

Adsorption of alkali atoms on transition metals has been intensively studied [1–11] due to important applications of these systems such as the preparation of low-work-function cathodes and the promotion of heterogeneous catalytic reactions. The surface structure of these systems has been discussed in detail and they have been related to work function and thermal desorption measurements.

The study of the electronic structure and chemical bonding, on one hand, has revealed that the alkali ions and their classic image charges induced in the substrate form a dipolar layer whose dipole moment variation with coverage has been explained using a reciprocal depolarization field in a Topping model formalism [1, 2]. The dipolar surface provides the explanation of the observed reduction of the work function with coverage. On the other hand, the interpretation of thermal desorption spectra requires an accurate modelling of adsorbate–adsorbate interactions, which, in the case of alkali atoms on transition metals, are of the long-range dipole–dipole type. The fitting of a model to complete sets of thermal desorption spectra for different coverages may provide a good tool for the determination of the interaction energy parameters. These, in turn, can be used to calculate the variation of dipole moment with coverage and, from it, the work function variation (which can be independently measured). This double check provides a severe test for any model.

The purpose of the present work is to use Monte Carlo simulation methods for the modelling of the complex system formed when alkali atoms are adsorbed on transition metals, to show how to obtain an estimation of interaction energies. For this study we have chosen the following systems: K/Ni(111), K/Pt(111) and K/Fe(111).

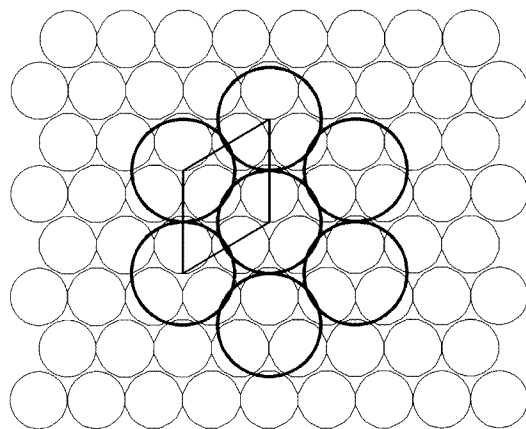
2. Model for K on transition metals (111) face

K adsorbs on different sites of the (111) surface, with multilayer formation at high coverages. Adsorption on threefold coordinated sites and on top sites has been observed in different adsorbate structures [11].

LEED patterns observed for K/Pt(111) [4, 10] show an ordered $\sqrt{3} \times \sqrt{3} R30^\circ$ structure at a potassium coverage of approximately one-third where saturation of the first layer occurs. For K/Ni(111) the situation is more complex, but again at saturation coverages around one-third a hexagonal close packed structure appears with some frozen-in disorder [19]. For K/Fe(111) the saturation coverage is again found to be very close to one-third but at that coverage no ordered structure is observed [1].

In some cases K adsorbs on transition metals forming even incommensurate structures [20].

Since our simulations will not be critically dependent upon the exact adsorption sites, but mainly on the number of neighbours each K atom will have, and in order to be consistent with the saturation coverage of one-third generally found, we assume for the adsorbate a triangular lattice (a K atom may have six nearest neighbours), where each K covers three substrate atoms (figure 1). An equivalent triangular lattice for K could be drawn using on top adsorption sites.



$$\sqrt{3} \times \sqrt{3} R 30^\circ$$

$$\Theta_K = 0.33$$

Figure 1. The structure of adsorbed potassium on Ni(111) showing first-, second- and third-order neighbours.

As generally accepted we consider that the adsorbed K atoms interact through a dipole–dipole repulsive force [12]. Given that this kind of interaction is a long-range one we approximate it by placing a cut-off at the fourth-order neighbour and replace true interaction energies by effective ones within that range. We define the interaction parameters as V_i^k , representing the interaction energy between a potassium atom at site i and one at site j (within the l th layer) which are k th-order neighbours.

As we already mentioned, it is absolutely necessary to take into account that the dipole moment of the dipolar layer decreases with coverage. This produces an attenuation of interaction parameters which vary from point to point on the surface according to the local

density of adsorbed atoms. We incorporate this into the model by introducing an attenuation function $\varphi_l(N_i)$ which depends on the local coverage around site i , N_i , and will, in general, be different for each adsorbed layer l . Given the atomic dimensions of K and the substrate, N_i can only take the values 0, 1, . . . , 6 up to third-order neighbours from an occupied site i .

Since our goal is to analyse thermal desorption spectra, we can write for the energy of an alkali atom adsorbed on site i in layer l :

$$E_l^i = E_{0l} + \sum_{k=1}^3 \sum_{(j,i)^k} V_l^k n_j \varphi_l(N_i) \quad (1)$$

where E_{0l} is the energy from any site in layer l at zero coverage ($E = 0$ corresponds to the gas phase), n_j is the occupation number of site j ($n_j = 0$ if empty, $n_j = 1$ if occupied) and the notation $(j, i)^k$ means that the summation must be taken over those sites j who are k th-order neighbours of site i .

The second term in the right-hand side of (1) represents the adsorbate–adsorbate interaction energy, Er_l^i , ‘seen’ by a particle adsorbed at site i in layer l . This term is strongly dependent on the spatial correlations between adsorbed particles, making exact analytical solutions for the desorption kinetics hopeless and the mean-field approximations too crude. For this reason we use Monte Carlo simulation to study the behaviour of the proposed model. We refer the reader to [13–15] for the details of the Monte Carlo simulation algorithm for thermal desorption. Given the desorption energy through (1), the desorption probability per unit time for a particle adsorbed at site i in layer l is given by

$$P_d^i = \nu \exp(-E_l^i/RT) \quad (2)$$

where R is the gas constant, T the temperature and ν the pre-exponential factor which we fix to the standard value of 10^{13} s^{-1} .

In our simulation the substrate is represented by a hexagonal lattice of M sites ($M \approx 10^5$) with periodic boundary conditions.

At a fixed temperature, each uncovered adsorbed atom is tested for desorption (this means that desorption is allowed to take place from different layers at the same time) and mean values are taken over 100 similar lattices. After all uncovered particles have been tested, a thermalization procedure is applied, by attempting to exchange randomly chosen pairs of adatoms and vacant sites, in order to keep the system in thermodynamic equilibrium.

Temperature is raised by very short intervals ΔT such that the coverage variation in each interval is small, i.e. if N_d atoms are desorbed between T and $T + \Delta T$, then $N_d/M \ll \theta$, where θ is the coverage at temperature T . Within each temperature interval, the following mean values are calculated:

- (i) N_d and the desorption rate $N_d/\Delta T$;
- (ii) the mean true adsorbate–adsorbate interaction energy

$$Er_l(\theta) = \frac{1}{N_d} \left(\sum_{i=1}^{N_d} Er_l^i \right); \quad (3)$$

- (iii) the mean unattenuated interaction energy

$$V_l(\theta) = \frac{1}{N_d} \left(\sum_{i=1}^{N_d} \sum_{k=1}^3 \sum_{(j,i)^k} V_l^k n_j \right); \quad (4)$$

- (v) the mean attenuation factor

$$f_l(\theta) = Er_l(\theta)/V_l(\theta). \quad (5)$$

These mean values are not really measurable quantities, however they are necessary to obtain the variation of dipole moment and work function with coverage, as will be shown in section 4.

3. Analysis of thermal desorption spectra

TPD spectra for K/Ni(111), K/Pt(111) and K/Fe(111) systems were simulated for different initial K coverages using the interaction energy and the attenuation factor as free parameters. In order to be rigorous, since a depolarization effect is present, the parameter E_{0l} ($l = 1, 2, \dots$), and very specially E_{01} , which represents the ‘chemical’ bond between the K dipole and the substrate, should also be considered to vary with coverage. Of course, this would complicate the model to a much bigger extent. However, the fact that considering constant E_{0l} values leads to good fits of desorption spectra and, at the same time, the attenuation factor, leads to a good agreement with the variation of work function with coverage in section 4 makes our simplifying approximation acceptable.

3.1. K/Ni(111)

Figure 2(a) shows experimental spectra obtained by Resch *et al* [16] for different initial potassium coverages on Ni(111). Alkali atoms were deposited on the substrate at 240 K and the temperature was raised at a rate of 10 K s⁻¹. The increase of desorption temperature with decreasing initial coverage is a consequence of the strong repulsive interactions. Multilayers are formed at high coverages and desorb in clearly distinguished peaks around 440 K. Desorption occurs in a very wide range of temperatures with a large plateau at low coverages. This feature can only be reproduced by considering the attenuation factor, i.e. it is a consequence of the decrease of the polarization of adsorbed atoms with increasing coverage.

Simulation results shown in figure 2(b) correspond to the set of parameters $E_{01} = -60.5$, $E_{02} = E_{03} = -28$, $V_1^1 = 2.73$, $V_1^2 = 1.43$, $V_1^3 = 1$, $V_2^1 = V_3^1 = 1.85$, $V_2^2 = V_3^2 = 0.97$, $V_2^3 = V_3^3 = 0.68$ (kcal mol⁻¹), and the attenuation function shown in figure 3(a). The attenuation factor describes the depolarization effect, which is strong at low coverages for the first layer and decays slowly after half-monolayer coverage, being null for the second layer.

Figure 3(b) shows the desorption energy $E_d(\theta)$ and the unattenuated interaction energy $V(\theta)$ for the first layer. The desorption energy undergoes a considerable change, from 60 to 28 kcal mol⁻¹ due to the dipole interaction energy, which corresponds to the large shift in peak temperatures (figure 2) from 950 K to around 500 K.

Predictions of the model for up to 3 ML coverages are shown, for completeness, in figure 4. Notice that, according to the sublimation energy of potassium of ≈ 20 kcal mol⁻¹ [4], one would expect desorption in the multilayer region to start at temperatures much higher than 100 K. However, according to the model, at a full layer lateral interactions V_l^k decrease the desorption energy from the multilayer from 28 to around 10 kcal mol⁻¹, thus allowing desorption at such a low temperature. The multiple peaks are now a consequence of the high lateral interactions compared to E_{02} and E_{03} . We cannot say that the model will still be valid at such high coverage, since unfortunately there are no experimental data to compare with. In fact, it would be interesting to determine whether repulsive K–K interactions due to the dipole moment could survive up to the third adsorbed layer.

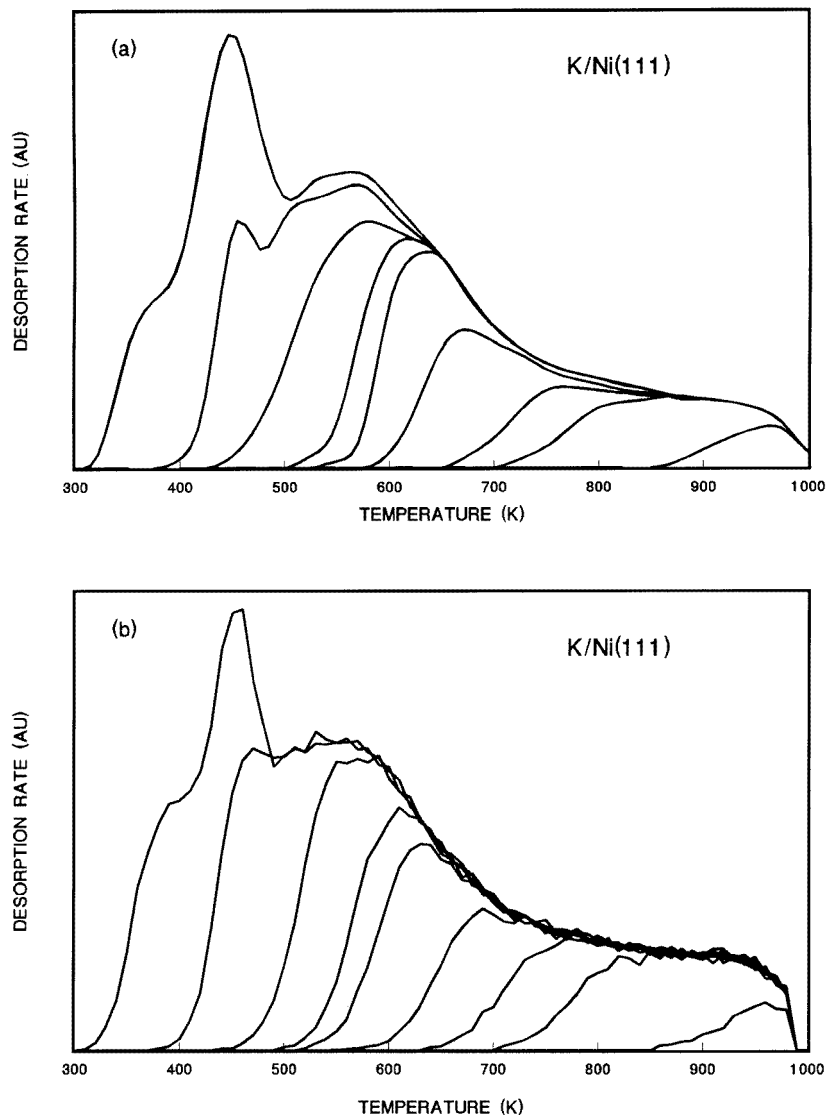


Figure 2. (a) Experimental thermal desorption spectra of K from the Ni(111) surface (from [16]). The initial K coverages for curves from left to right are 1.25, 1.0, 0.76, 0.59, 0.52, 0.38, 0.28, 0.20 and 0.05. (b) Simulated TPD spectra of K/Ni(111). The heating rate was 10 K s⁻¹. The initial K coverages for curves from left to right are 1.25, 1.0, 0.76, 0.59, 0.52, 0.38, 0.28, 0.20, and 0.05.

3.2. K/Pt(111)

Experimental desorption spectra obtained by Garfunkel and Somorjai [4] with a heating rate of 30 K s⁻¹ are shown in figure 5(a), while figure 5(b) shows the spectra simulated with $E_{01} = -64$, $E_{02} = -23$, $V_1^1 = 2.52$, $V_1^2 = 2.34$, $V_1^3 = 2.06$, $V_2^1 = V_2^2 = V_2^3 = 0$ (kcal mol⁻¹), and the attenuation factor shown in figure 6(a). The general behaviour is similar to that already discussed for K/Ni(111). In this case, however, experimental data

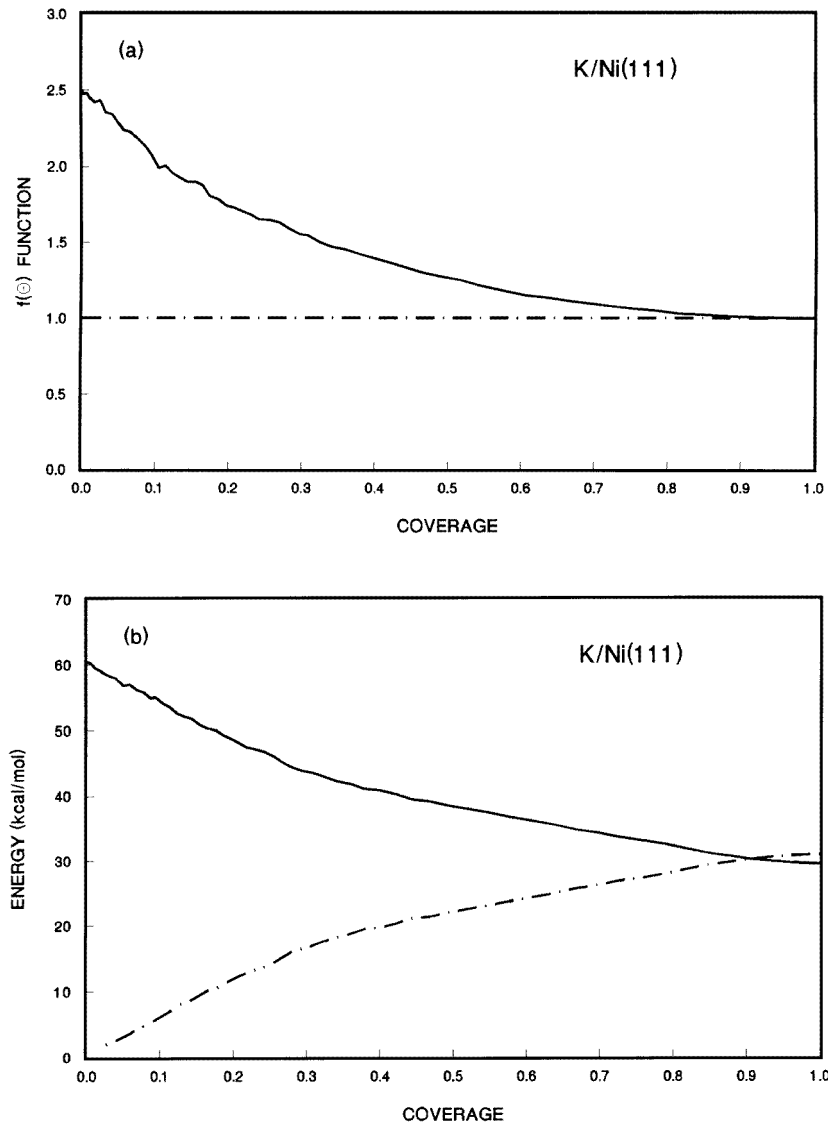


Figure 3. (a) The attenuation function for K/Ni(111): $l = 1$, first layer (solid line); $l = 2$ and 3, second and third layers (dot-dash line). (b) K desorption energy (solid line) and K-K unattenuated interaction energy (dot-dash line) as functions of coverage on the Ni(111) surface.

for the desorption energy (from the first layer) are also available from [4] and an excellent agreement with $E_d(\theta)$ is shown in figure 6(b).

3.3. K/Fe(111)

TPD spectra obtained by Lee *et al* [1] with a heating rate of 10 K s^{-1} ($\theta < 1 \text{ ML}$) are shown in figure 7(a) and simulated results are shown in figure 7(b). The latter correspond to parameter values $E_{01} = -53$, $V_1^1 = 2.5$, $V_1^2 = 1.3$ and $V_1^3 = 0.90$ (energies in kcal mol^{-1})

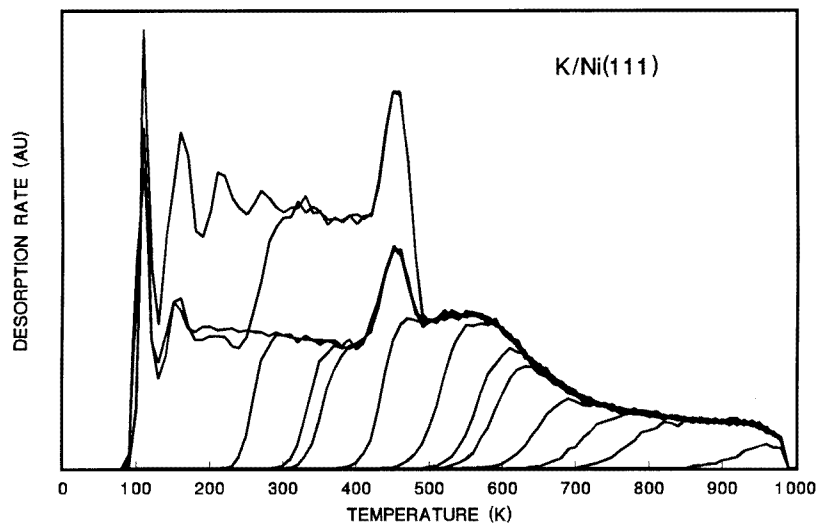


Figure 4. Simulated TPD spectra of K/Ni(111) for K coverage up to 3 ML. The heating rate was 10 K s^{-1} . The initial coverages for curves from left to right are 2.9, 2.5, 2.0, 1.5, 1.3, 1.25, 1.0, 0.76, 0.58, 0.52, 0.38, 0.28, 0.2, and 0.05.

and the attenuation factor shown in figure 8(a). The energy E_{01} agrees with the values reported in [1] and [17]. The desorption and interaction energies are shown in figure 8(b). The behaviour is again similar to that for K/Ni(111).

4. Calculation of the dipole moment and work function

Effects of a depolarization field on adsorbate–adsorbate interactions have been discussed by several authors [2, 17]. Assuming the adsorbate as a polarizable entity with a coverage dependent dipole moment $\mu(\theta)$ and a constant polarizability α , and using the Topping model, it can be shown that

$$\mu(\theta) = \mu_0 / (1 + 9\alpha\theta^{3/2}) \quad (6)$$

where μ_0 is the dipole moment of an isolated adatom, and that the dipole interaction energy $E_r^*(\theta)$ is given by

$$E_r^*(\theta) = 9\mu^2(\theta)\theta^{3/2} = 9\mu_0^2\theta^{3/2} / (1 + 9\alpha\theta^{3/2})^2 \quad (7)$$

(distances are assumed to be measured in units of the size of an elementary cell).

On the other hand the variation of work function with coverage, $\Delta\phi(\theta)$, can be obtained in terms of $\mu(\theta)$ through the Helmholtz equation [1, 2] and the Topping model as

$$\Delta\phi = 2\pi\mu(\theta)\theta. \quad (8)$$

Comparison of (7) with simulated interaction energy (3) allows the determination of μ_0 and α via least-squares minimization (the agreement between $E_r(\theta)$ and $E_r^*(\theta)$ is shown in figure 9 just for K/Ni(111)) and then $\mu(\theta)$ and $\Delta\phi(\theta)$ can be predicted, through (6) and (8), for each system (figures 10–12).

For the K/Fe(111) system, independent measurements of $\mu(\theta)$ and $\Delta\phi(\theta)$ are available [1, 7] and these experimental data are compared to simulation predictions in figure 12, showing a satisfactory agreement.

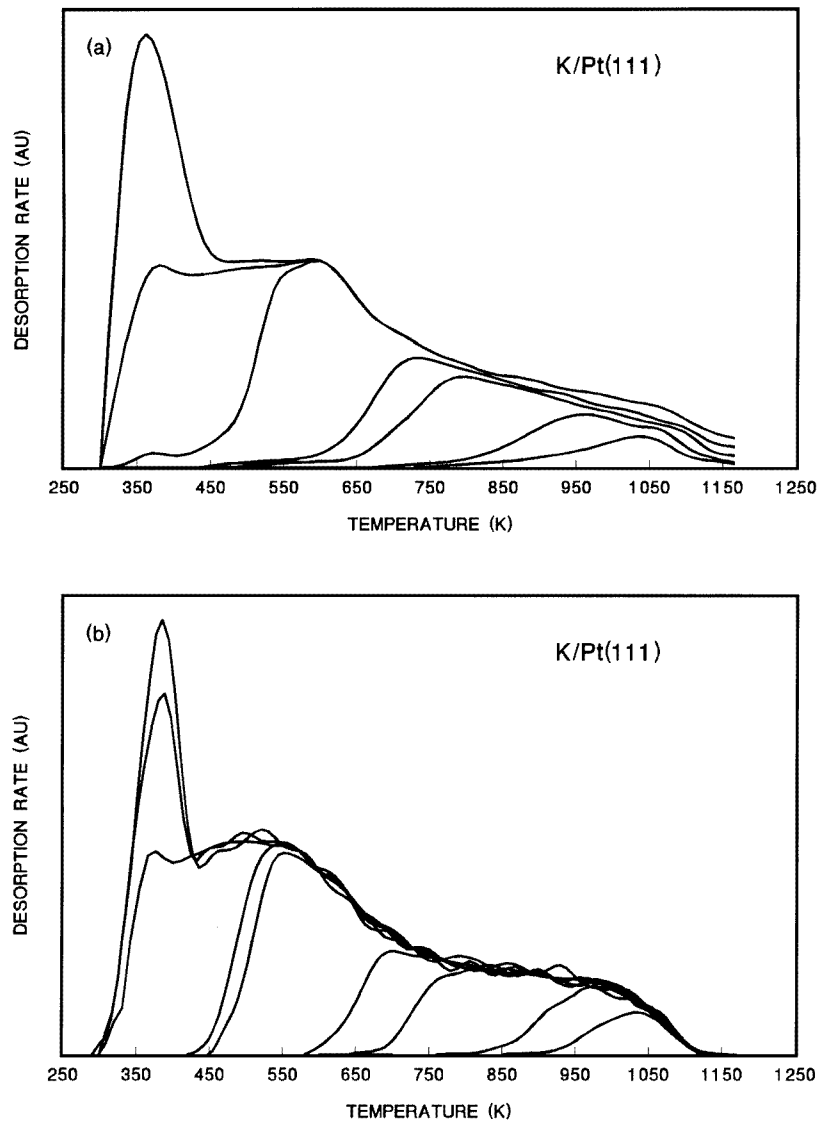


Figure 5. (a) Experimental thermal desorption for various amounts of K from the Pt(111) surface (from [4]). The initial K coverages for curves from left to right are 1.21, 1.0, 0.7, 0.36, 0.27, 0.11, and 0.05. (b) Simulated TPD spectra of K/Pt(111). The heating rate was 30 K s^{-1} . The initial K coverages for curves from left to right are 1.13, 1.1, 1.0, 0.7, 0.66, 0.36, 0.27, 0.11, and 0.05.

5. Conclusions

It has been shown that the thermal desorption of alkali atoms (in our case potassium) from the transition metal (111) face is strongly dependent on spatial correlations between adatoms, since they interact through long-range dipole-dipole forces whose intensity decreases with coverage due to depolarization. This complicates the microscopic description of the system

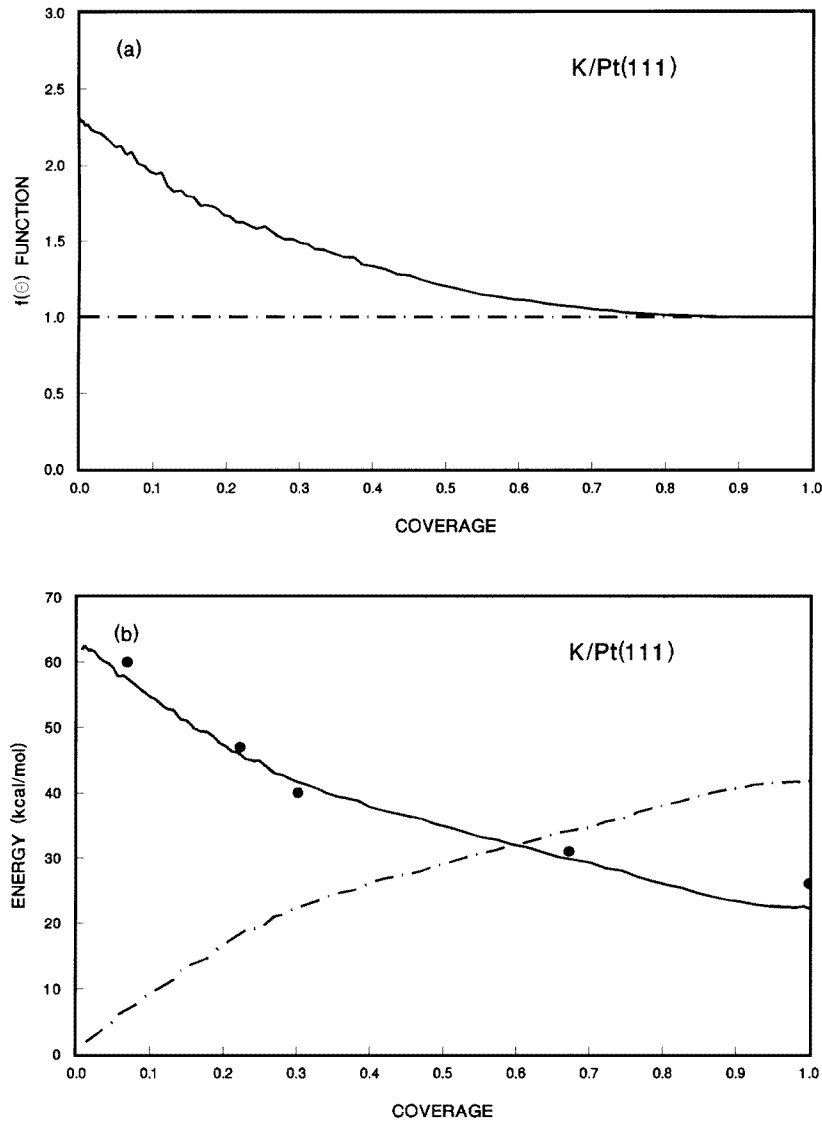


Figure 6. (a) The attenuation function for K/Pt(111): $l = 1$, first layer (solid line); $l = 2$, second layer (dot-dash line). (b) K desorption energy (solid line) and K-K unattenuated interaction energy (dot-dash line) as functions of coverage on the Pt(111) surface. Experimental data (full circles) for K desorption energy are from [4].

even though we place a cut-off for interactions farther than third-order neighbours. The statistical mechanics formulation of the problem leads to the fundamental equation for the desorption rate [18]:

$$\frac{d\theta}{dt} = -k_d^0 \sum_{\alpha} P_{A,\alpha} \exp[-(E_{\alpha}^* - E_{\alpha})/RT] \theta \quad (9)$$

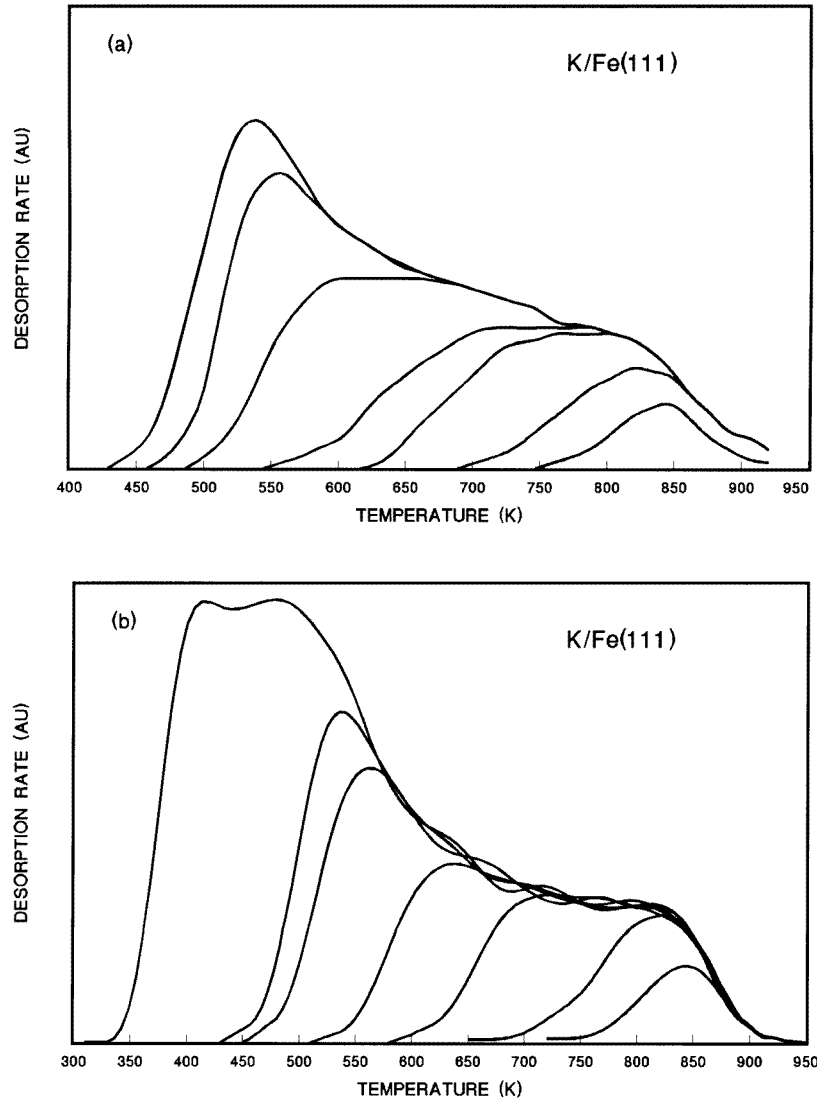


Figure 7. (a) Experimental thermal desorption for various amounts of K from the Fe(111) surface (from [1]). The initial K coverages for curves from left to right are 0.57, 0.5, 0.36, 0.23, 0.18, 0.11, and 0.05. (b) Simulated TPD spectra of K/Fe(111). The heating rate was 10 K s^{-1} . The initial K coverages for curves from left to right are 1.0, 0.57, 0.5, 0.34, 0.23, 0.11, and 0.05.

where k_d^0 is the desorption rate constant in ideal conditions, $P_{A,\alpha}$ is the probability that an adsorbed atom A has an environment α , E_α and E_α^* are the interaction energies for the atom and the activated complex, respectively, with the environment.

If spatial correlations among adatoms are strong, as in our case, this equation cannot be solved analytically and the mean-field and quasi-chemical approximations are too rough when long-range interactions must be taken into account. Monte Carlo simulation is the only suitable method in such a situation.

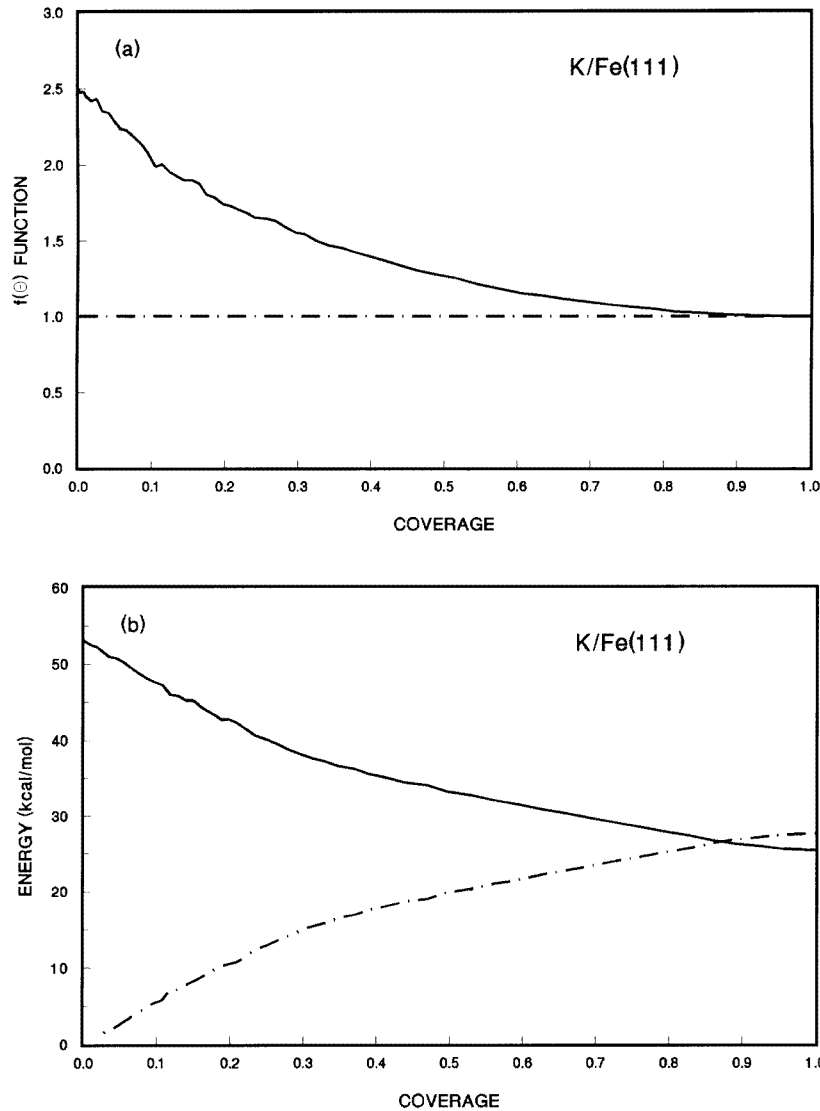


Figure 8. (a) Attenuation function for K/Fe(111): $l = 1$, first layer (solid line); $l = 2$, second layer (dot-dash line). (b) K desorption energy (solid line) and K-K unattenuated interaction energy (dot-dash line) as a function of coverage on the Fe(111) surface.

On the other hand, one could consider in place of (9) an empirical Arrhenius equation:

$$\frac{d\theta}{dt} = -\nu(\theta) \exp(-E_d(\theta)/RT) \theta^n \quad (10)$$

where $\nu(\theta)$ and $E_d(\theta)$ are the apparent preexponential factor and activation energy for desorption and n is the apparent reaction order. This approach is more familiar but its advantage is doubtful. In fact (i) the number of fitting parameters is not less than those included in (9) (here we have two functions $\nu(\theta)$ and $E_d(\theta)$ and one parameter, n), and (ii) we are now dealing with 'apparent' parameters instead of direct physical microscopic

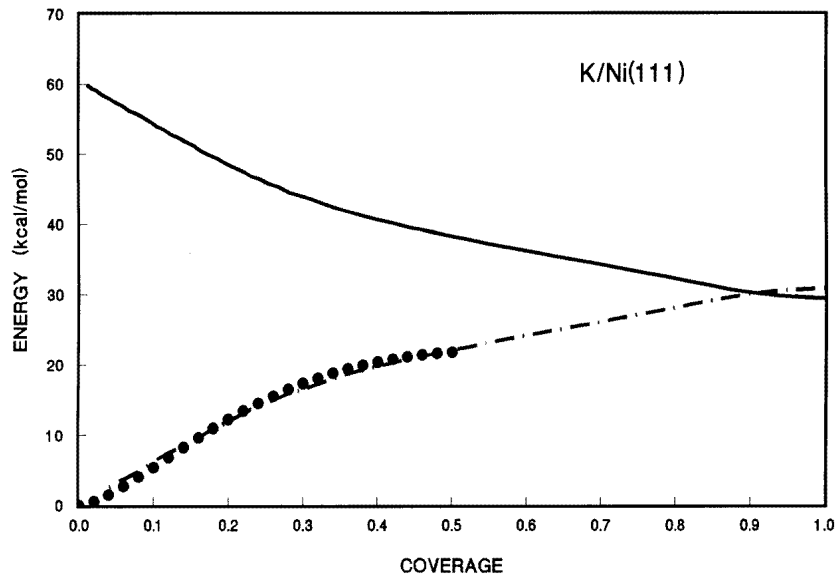


Figure 9. A comparison between $E_r(\bullet)$ and E_r^* ($-\cdot-$) as a function of θ for the system K/Ni(111); the full line represents the desorption energy.

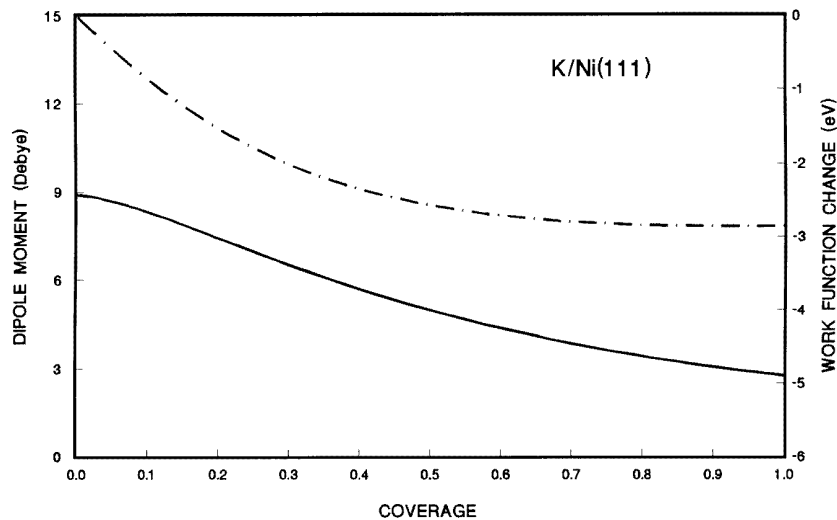


Figure 10. Dipole moment μ (solid line) and work function change $\Delta\phi$ (dot-dash line) as a function of coverage for K/Ni(111) from simulation. The parameters obtained by the interaction energy fit were dipole moment at zero coverage $\mu_0 = 8.9$ Debye and polarizability $\alpha = 15.7 \times 10^{-24} \text{ cm}^3$ for $N_{sat} = 5.5 \times 10^{14} \text{ atoms cm}^{-2}$.

parameters (interaction energies).

Even though the number of free parameters used in our Monte Carlo simulations to fit thermal desorption spectra is high, so is the number of curves which are simultaneously fitted with the same set of parameters. Moreover the approach we used (microscopic

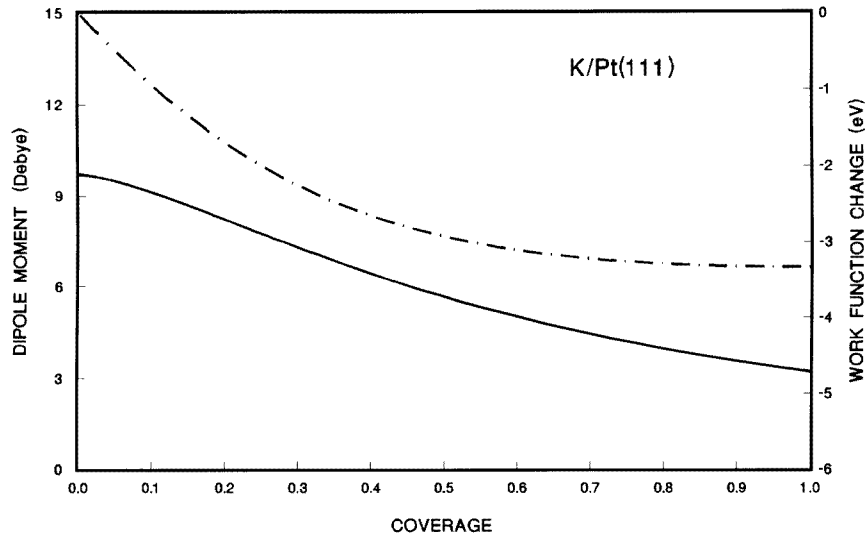


Figure 11. Dipole moment μ (solid line) and work function change $\Delta\phi$ (dot-dash line) as a function of coverage for K/Pt(111) from simulation. The parameters obtained by the interaction energy fit were dipole moment at zero coverage $\mu_0 = 9.7$ Debye and polarizability $\alpha = 14.2 \times 10^{-24} \text{ cm}^3$ for $N_{sat} = 5.5 \times 10^{14} \text{ atoms cm}^{-2}$.

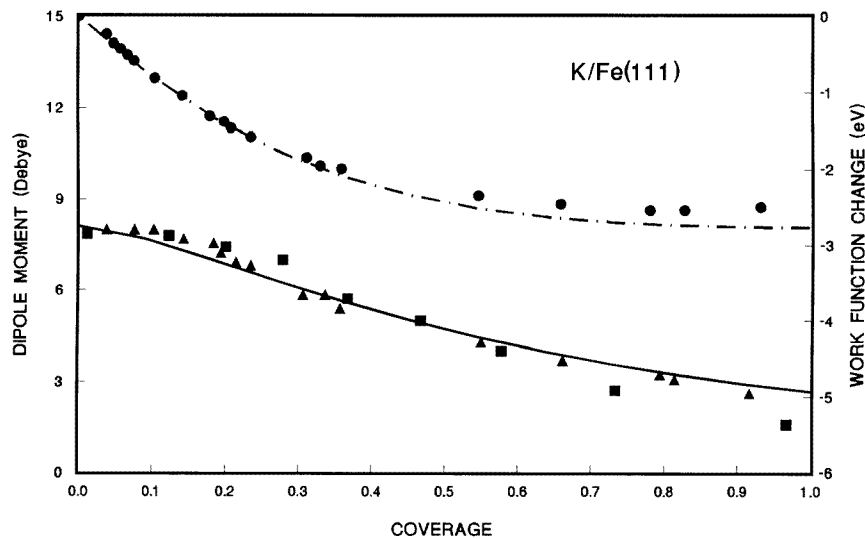


Figure 12. Dipole moment μ (solid line) and work function change $\Delta\phi$ (dot-dash line) as a function of coverage for K/Fe(111) from simulation. The parameters obtained by the interaction energy fit were dipole moment at zero coverage $\mu_0 = 8.1$ Debye and polarizability $\alpha = 14.4 \times 10^{-24} \text{ cm}^3$ for $N_{sat} = 5.5 \times 10^{14} \text{ atoms cm}^{-2}$. Experimental dipole moments are from [7] (squares) and [1] (triangles) and work function change [1] (circles).

description) allows the calculation of interactions and their attenuation with coverage and these calculations, in turn, can be related to independent measurements of dipole moment and work function, providing a double-check of the proposed model.

The procedure could also be used the other way around, i.e. first to fit dipole moment and/or work function data obtaining interaction energies and then to use these to predict thermal desorption spectra.

Acknowledgments

This work was made possible by the support of the European Economic Community, through project ITDC-240, and of the Consejo Nacional de Investigaciones Científicas y Técnicas (CONICET) of Argentina.

References

- [1] Lee S B, Weiss M and Ertl G 1981 *Surf. Sci.* **108** 357
- [2] Desplat J L 1981 *Surf. Sci.* **109** 381
- [3] Crowell J E, Garfunkel E L and Somorjai G A 1982 *Surf. Sci.* **121** 303
- [4] Garfunkel E L and Somorjai G A 1982 *Surf. Sci.* **115** 441
- [5] Heskett D 1988 *Surf. Sci.* **199** 67
- [6] Bertolini J L, Delichere P and Massardier J 1985 *Surf. Sci.* **160** 531
- [7] Ertl G, Lee S B and Weiss M 1982 *Surf. Sci.* **114** 527
- [8] Luftman H S, Sun Y M and White J M 1984 *Appl. Surf. Sci.* **19** 82
- [9] Luftman H S, Sun Y M and White J M 1984 *Surf. Sci.* **141** 82
- [10] Benziger J and Madix R J 1980 *Surf. Sci.* **94** 119
- [11] Diehl R D and McGrath R 1996 *Surf. Sci. Rep.* **23** 43
- [12] Gerlach R L and Rhodin T N 1970 *Surf. Sci.* **19** 403
- [13] Binder K 1978 *Monte Carlo Methods in Statistical Physics (Topics in Current Physics 7)* (Berlin: Springer)
- [14] Sales J L and Zgrablich G 1987 *Surf. Sci.* **187** 1
Sales J L and Zgrablich G 1987 *Phys. Rev. B* **35** 9520
Fichthorn K A and Weinberg W H 1991 *Langmuir* **7** 2539
Meng B and Weinberg W H 1994 *J. Chem. Phys.* **100** 5280
- [15] Sales J L, Uñac R, Gargiulo M V, Bustos V and Zgrablich G 1996 *Langmuir* **12** 95
- [16] Resch C, Zhukov V, Lugstein A, Berger H F, Winkler A and Rendulic K D 1993 *J. Chem. Phys.* **177** 421
- [17] Albano E 1986 *J. Chem. Phys.* **85** 1044
- [18] Zhdanov V P 1991 *Elementary Physicochemical Processes on Solid Surfaces* (New York: Plenum)
- [19] Müller K, Besold G and Heinz K 1989 *Alkali Adsorption on Metal and Semiconductors* ed H P Bonzel, A M Bradshaw and G Ertl (Amsterdam: Elsevier)
- [20] Diehl R D and McGrath R 1995 *Surf. Rev. Lett.* **2** 387